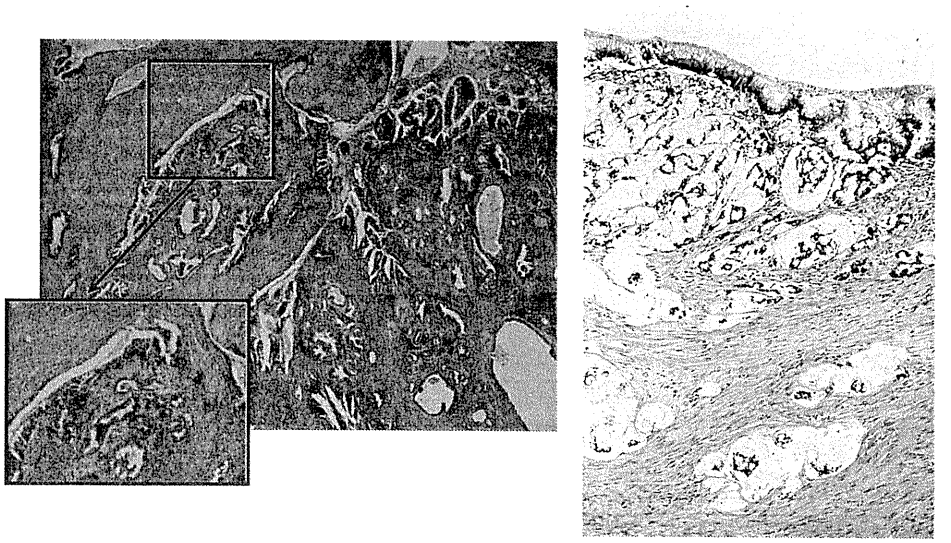

From IPMN to tubular carcinoma From IPMN to mucinous carcinoma

FIGURE 1. Histological transition from IPMN to tubular carcinoma or mucinous carcinoma.

TABLE 1. Intraductal Papillary Mucinous Neoplasm, PDAC Derived From IPMN, and PDAC Concomitant With IPMN

IPMN	582 cases
Adenoma	381 cases
Carcinoma	201 cases
Noninvasive	157 cases
Minimally invasive	44 cases
PDAC derived from IPMN	122 cases
PDAC concomitant with IPMN	31 cases
PDAC undetermined derived from IPMN or concomitant with IPMN	30 cases
Total	765 cases

TABLE 2. Clinical Features of Patients With PDAC, PDAC Derived From IPMN, and PDAC Concomitant With IPMN (Overall)

	PDAC	PDAC Derived From IPMN		PDAC Concomitant With IPMN	
	(n = 7605)	(n = 122)	*P*	(n = 31)	*P*
Age,* mean (SD), yr	63.5 (9.9)	66.5 (8.4)	<0.001	67.1 (8.2)	0.021
Sex,† n (%)					
Male	4674 (61.5)	77 (63.1)	0.67	21 (67.7)	0.457
Female	2931 (38.5)	45 (36.9)		10 (32.3)	
Follow-up duration,* mean (SD), mo	17.1 (22.0)	36.7 (36.0)	<0.001	37.3 (36.9)	<0.001

P value compared with PDAC.
*Two-sample *t* test.
†χ^2 test.

Undetermined Whether PDAC Is Derived From IPMN or Concomitant With IPMN

Intraductal papillary mucinous neoplasm and PDAC are evident, but whether PDAC was derived from IPMN or whether PDAC was concomitant with IPMN could not be determined because there was no histological transition between the 2 diseases. The histological transition might not be evident (1) because serial stepwise section examination of the resected specimens was not done in all the cases, (2) because the transition might have disappeared because of the extensive and massive growth of PDAC, or (3) because the 2 diseases developed independently and collided with each other. Thus, such cases were considered as undetermined whether PDAC was derived

TABLE 3. Comparison Among IPMN Types and IPMN, PDAC Derived From IPMN, and PDAC Concomitant With IPMN

	Main Duct (+Mixed) Type, n (%)	Branch Duct Type, n (%)	*P*
IPMN (n = 582)	181 (31.1)	401 (68.9)	—
PDAC derived from IPMN (n = 122)	61 (50.0)	61 (50.0)	<0.001
Tubular adenocarcinoma (n = 81, 66.4%)	38 (46.9)	43 (53.1)	0.004
Mucinous carcinoma (n = 41, 33.6%)	23 (56.1)	18 (43.9)	0.001
PDAC concomitant with IPMN (n = 31)	3 (9.6)	28 (90.4)	0.012
Tubular adenocarcinoma (n = 31, 100%)	3 (9.6)	28 (90.4)	0.012
Mucinous carcinoma (n = 0, 0.0%)	0 (0)	0 (0)	NA

P value compared with IPMN.
NA indicates not available.

TABLE 4. Clinicopathological Findings of PDAC, PDAC Derived From IPMN, and PDAC Concomitant With IPMN (Overall)

		PDAC (n = 7605)		PDAC Derived From IPMN (n = 122)			PDAC Concomitant With IPMN (n = 31)		
		n	%	n	%	*P*	n	%	*P*
Histological diagnosis	Tubular adenocarcinoma	7484	98.4	60	69.0	<0.001	20	100	0.57
	Mucinous adenocarcinoma	121	1.6	26	29.9		0	0.0	
	Tubular + mucinous	0	0.0	1	1.1		0	0.0	
	Unknown	0		35			0		
Location	Head	5204	68.6	77	67.0	0.222	14	46.7	<0.001
	Body	974	12.8	10	8.7		11	33.3	
	Tail	420	5.5	9	7.8		5	16.7	
	All segments of pancreas	115	1.5	4	3.5		0	0.0	
	Two segments of pancreas	868	11.4	15	13.0		1	3.3	
	Unknown	24		7			1		
TS	TS1	882	12.0	9	7.4	0.005	15	48.4	<0.001
	TS2	3921	53.6	65	53.7		12	38.7	
	TS3	1837	25.1	25	20.7		4	12.9	
	TS4	681	9.3	22	18.2		0	0.0	
	Unknown	284		1			0		
T	Tis	0	0.0	0	0.0	<0.001	2	6.5	<0.001
	T1	229	3.2	8	6.6		9	29.0	
	T2	281	3.9	27	22.1		0	0.0	
	T3	1915	26.8	72	59.0		14	45.2	
	T4	4714	66.0	15	12.3		6	19.4	
	Unknown	466		0			0		
N	N0	2319	33.7	65	53.3	<0.001	14	45.2	0.01
	N1	1518	22.1	39	32.0		12	38.7	
	N2	1399	20.3	15	12.3		4	12.9	
	N3	1642	23.9	3	2.5		1	3.2	
	Unknown	727		0			0		
M	M (−)	5480	72.4	118	96.7	<0.001	31	100	0.001
	M (+)	2092	27.6	4	3.3		0	0.0	
	Unknown	33		0			0		
Stage	0	0	0.0	0	0.0	<0.001	2	6.5	<0.001
	I	146	2.2	6	4.9		8	25.8	
	II	167	2.5	26	21.3		1	3.2	
	III	1278	19.0	57	46.7		10	32.3	
	IVA	2250	33.4	22	18.0		8	25.8	
	IVB	2887	42.9	11	9.0		2	6.5	
	Unknown	877		0			0		

P value compared with PDAC.

from IPMN or PDAC was concomitant with IPMN and were excluded from further comparisons to examine the details of each discrete condition.

The clinicopathological data of 765 patients who underwent surgical resection for IPMN were collected from the following 7 representative Japanese institutions:

TABLE 5. Median Survival of PDAC, PDAC Derived From IPMN, and PDAC Concomitant With IPMN (Overall)

PDAC (n = 7605)		PDAC Derived From IPMN (n = 122)		PDAC Concomitant With IPMN (n = 31)		Results of the Log-Rank Test (*P*)	
n	MST, mo	n	MST, mo	n	MST, mo	PDAC vs PDAC Derived From IPMN	PDAC vs PDAC Concomitant With IPMN
7359	12	122	46	31	57	<0.001	<0.001

Department of Surgery 1, School of Medicine, University of Occupational and Environmental Health, Japan, Kitakyushu, Japan
Department of Surgery and Oncology, Graduate School of Medical Sciences, Kyushu University, Fukuoka, Japan.
Department of Gastroenterological Surgery, Tokyo Women's Medical University School of Medicine, Tokyo, Japan,
Center for Gastroenterology, Teine-Keijinkai, Sapporo, Japan,
Department of Gastroenterological Surgery, Aichi Cancer Center, Nagoya, Japan
Department of Gastroenterology, University of Tokyo, Tokyo, Japan, and
Department of Surgery, Tokai University School of Medicine, Isehara, Japan

We had 4 committee meetings where we reviewed the radiologic images and hematoxylin-eosin–stained sections of the patients and discussed the differentiation of the tumors and determined the diagnostic criteria. All 765 patients underwent surgery from February 1987 to February 2009. They consisted of 381 patients with intraductal papillary mucinous adenoma (IPMA) (49.8%), 201 with intraductal papillary mucinous carcinoma (26.3%) (157 with noninvasive IPMC and 44 with minimally invasive IPMC), 122 judged to have PDAC derived from IPMN (15.9%), 31 judged to have PDAC concomitant with IPMN (4.1%), and 30 for whom it could not be determined whether the PDAC derived from IPMN or was concomitant with IPMN (3.9%) (Table 1).

In addition, data from 7605 patients with PDAC who were registered in the JPS pancreatic cancer registry were obtained under the permission of the president of the JPS (Professor Masao Tanaka, MD, PhD, FACS, Department of Surgery and Oncology, Graduate School of Medical Sciences, Kyushu University, Fukuoka, Japan). These patients underwent surgical resection in 168 Japanese institutions from November 1971 to January 2005.

Data were analyzed following the *Classification of Pancreatic Carcinoma* published by the JPS (Second English Edition, 2003, Kanehara & Co, Ltd, Tokyo, Japan).[6] Statistical analyses were done by *t* test, χ^2 test, and log-rank test. The mean

TABLE 6. Clinicopathological Features and MST (Overall Cases)

		PDAC (n = 7605)			PDAC Derived From IPMN (n = 122)			PDAC Concomitant With IPMN (n = 31)		
		n	%	MST, mo	n	%	MST, mo	%	n	%	MST, mo
All cases		7605	100.0	12	122	100.0	46	100.0	31	100.0	57
Histological diagnosis	Tubular adenocarcinoma	7484	98.4	13	60	69.0	44	69.0	20	100	51
	Mucinous adenocarcinoma	121	1.6	31	26	29.9	55	29.9	0	0.0	NA
	Tubular + mucinous	0	0.0	NA	1	1.1	30	1.1	0	0.0	NA
	Unknown	0			35				0		
TS	TS1	882	12.0	29	9	7.4	38	7.4	15	48.4	59
	TS2	3921	53.6	14	65	53.7	42	53.7	12	38.7	24
	TS3	1837	25.1	10	25	20.7	54	20.7	4	12.9	12
	TS4	681	9.3	9	22	18.2	61	18.2	0	0.0	NA
	Unknown	284			1				0		
T	Tis	0	0.0	NA	0	0.0	NA	0.0	2	6.5	138
	T1	229	3.2	45	8	6.6	50	6.6	9	29.0	42
	T2	281	3.9	25	27	22.1	39	22.1	0	0.0	NA
	T3	1915	26.8	19	72	59.0	62	59.0	14	45.2	62
	T4	4714	66.0	10	15	12.3	35	12.3	6	19.4	24
	Unknown	466			0				0		
N	N0	2319	33.7	20	65	53.3	54	53.3	14	45.2	73
	N1	1518	22.1	14	39	32.0	31	32.0	12	38.7	54
	N2	1399	20.3	11	15	12.3	47	12.3	4	12.9	24
	N3	1642	23.9	9	3	2.5	24	2.5	1	3.2	NA
	Unknown	727			0				0		
M	M (−)	5480	72.4	16	118	96.7	47	96.7	31	100	57
	M (+)	2092	27.6	9	4	3.3	36	3.3	0	0.0	NA
	Unknown	33			0				0		
Stage	0	0	0.0	NA	0	0.0	NA	0.0	2	6.5	138
	I	146	2.2	57	6	4.9	47	4.9	8	25.8	36
	II	167	2.5	36	26	21.3	42	21.3	1	3.2	54
	III	1278	19.0	23	57	46.7	60	46.7	10	32.3	60
	IVA	2250	33.4	15	22	18.0	39	18.0	8	25.8	24
	IVB	2887	42.9	9	11	9.0	44	9.0	2	6.5	12
	Unknown	877			0				0		

follow-up period was determined when the final follow-up information was obtained. Mean follow-up period of the 7605 cases with PDAC was 17.1 months, that of the 122 cases with PDAC derived from IPMN was 36.7 months, and that of the 31 cases with PDAC concomitant with IPMN was 37.3 months (Table 2). Survival curves were made by the Kaplan-Meier method. $P < 0.05$ was considered statistically significant.

RESULTS

Clinicopathological Comparison Between PDAC and PDAC Derived From IPMN and Between PDAC and PDAC Concomitant With IPMN

The mean ages of patients with PDAC derived from IPMN and PDAC concomitant with IPMN was 66.5 ($P < 0.001$) and 67.1 ($P = 0.021$) years, respectively, both of which were significantly higher than the mean age of 63.5 years of the PDAC patients. The male-to-female ratio was approximately 60% in all 3 groups (Table 2). The IPMN in the cases of PDAC derived from IPMN was significantly more frequently of the main duct type than when IPMN was detected alone, and most IPMNs in PDAC concomitant with IPMN were of the branch duct type, which was not the case when patients presented with IPMN only. Concerning the histological type, approximately one-third of the cases of PDAC derived from IPMN (41/122) were mucinous carcinomas, although most of the cases of PDAC concomitant with IPMN (28/31) were tubular adenocarcinomas, similar to ordinary PDAC (Table 3). Approximately 30% of the cases of PDAC derived from IPMN were mucinous carcinomas, which was significantly more frequent than is observed in patients with PDAC alone ($P < 0.001$; Table 4). More than 50% of the lesions of PDAC concomitant with IPMN were located in the body or tail of the pancreas, whereas approximately 70% of PDAC ($P < 0.001$) and PDAC derived from IPMN ($P = 0.002$) were in the head of the pancreas. About 50% of the cases of PDAC concomitant with IPMN were of TS1 (≤2 cm) in size, whereas approximately 10% of PDAC ($P < 0.001$) and PDAC derived from IPMN ($P < 0.001$) were of TS1. Lymph node metastasis in PDAC was significantly more frequent and more extensive than

P for No. Cases			*P* for MST		
PDAC vs PDAC Derived From IPMN	PDAC vs PDAC Concomitant With IPMN	PDAC Derived From IPMN vs PDAC Concomitant With IPMN	PDAC vs PDAC Derived From IPMN	PDAC vs PDAC Concomitant With IPMN	PDAC Derived From IPMN vs PDAC Concomitant With IPMN
			<0.001	<0.001	0.808
<0.001	0.57	0.016	<0.001	0.003	0.354
			0.354	NA	NA
			NA	NA	NA
0.005	<0.001	<0.001	0.888	0.337	0.19
			<0.001	0.031	0.116
			<0.001	0.028	0.689
			<0.001	NA	NA
			<0.001	0.002	0.127
<0.001	<0.001	<0.001	NA	NA	NA
			0.732	0.301	0.815
			0.404	NA	NA
			<0.001	0.104	0.14
			0.001	0.007	0.831
<0.001	0.01	0.87	<0.001	0.136	0.601
			<0.001	0.015	0.404
			<0.001	0.036	0.369
			0.223	0.280	0.333
<0.001	0.001	0.307	<0.001	0.001	0.789
			0.017	NA	NA
<0.001	<0.001	<0.001	NA	NA	NA
			0.676	0.141	0.917
			0.986	0.957	0.625
			0.001	0.717	0.075
			<0.001	0.018	0.778
			<0.001	0.075	0.67

(Table 6 continued from previous page. Data read horizontally)

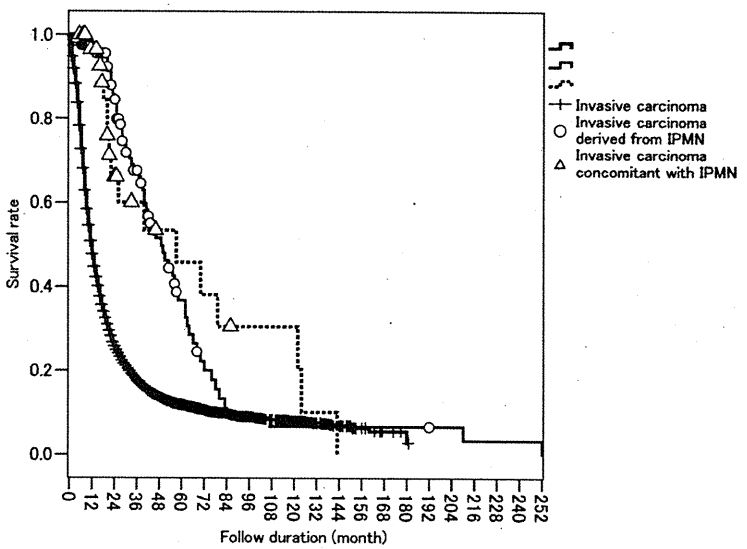

	survival rate		
	1-year	3-year	5-year
PDAC	51%	19%	12%
PDAC derived from IPMN	97%	68%	37%
PDAC concomitant with IPMN	97%	61%	46%

* p<0.001

FIGURE 2. Survival curves of PDAC, PDAC derived from IPMN, and PDAC concomitant with IPMN (overall).

in patients with PDAC derived from IPMN and PDAC concomitant with IPMN. Distant metastasis was also more frequent in PDAC than in PDAC derived from IPMN and PDAC concomitant with IPMN. In addition, the stage at the time of the diagnosis of PDAC was more advanced than in patients diagnosed with PDAC derived from IPMN and PDAC concomitant with IPMN.

The median survival times (MSTs) of the 122 patients with PDAC derived from IPMN and of 31 with PDAC concomitant with IPMN were 46 and 57 months, respectively, both of which were significantly longer than the 12 months of the 7605 patients with PDAC (Table 5). The MST of the 7605 patients with PDAC of the tubular type was 13 months, which was significantly shorter than the 44 months of the 122 patients with PDAC derived from IPMN ($P < 0.003$) and 51 months of the 31 patients with PDAC concomitant with IPMN ($P = 0.016$) (Table 6). The MSTs of patients with PDAC of TS1, TS2, TS3, and TS4 were significantly shorter than those of patients with PDAC derived from IPMN and PDAC concomitant with IPMN. The MSTs of patients with PDAC of stage I or II were similar to those of patients with PDAC derived from IPMN and PDAC concomitant with IPMN. However, the MSTs of patients with stage III, IVA, and IVB PDAC were significantly shorter than those of patients with PDAC derived from IPMN and concomitant with IPMN. The survival curve of the patients with PDAC was more unfavorable than that for patients with PDAC derived from IPMN ($P < 0.001$) and with PDAC concomitant with IPMN ($P < 0.001$) (Fig. 2). The 1-, 3-, and 5-year survival rates of PDAC were 51%, 19%, and 12%, respectively, all of which were significantly shorter than 97%, 68%, and 37% of patients with PDAC derived from IPMN and the 97%, 61%, and 46% of patients with PDAC concomitant with IPMN.

TABLE 7. Clinical Features of PDAC, PDAC Derived From IPMN, and PDAC Concomitant With IPMN (TS2 or TS3)

	PDAC	PDAC Derived From IPMN		PDAC Concomitant With IPMN	
	(n = 5758)	(n = 90)	*P*	(n = 16)	*P*
Age,* mean (SD), yr	63.6 (9.9)	66.0 (8.7)	0.012	69.4 (6.4)	0.002
Sex†					
Male	3520 (61.1)	60 (66.7)	0.285	11 (68.8)	0.532
Female	2238 (38.9)	30 (33.3)		5 (31.3)	
Follow-up duration,* mean (SD), mo	15.8 (20.0)	34.7 (34.9)	<0.001	16.4 (7.5)	0.759

P value compared with PDAC.
*Two-sample *t* test.
†χ^2 test.

TABLE 8. Clinicopathological Findings of PDAC, PDAC Derived From IPMN, and PDAC Concomitant With IPMN (TS2 or TS3)

		IDC (n = 5758)		IDC Derived From IPMN (n = 90)			IDC Concomitant With IPMN (n = 16)		
		n	%	n	%	*P*	n	%	*P*
Histological diagnosis	Tubular adenocarcinoma	5686	98.7	51	73.9	<0.001	10	100	0.722
	Mucinous adenocarcinoma	72	1.3	17	24.6		0	0.0	
	Tubular + mucinous	0	0.0	1	1.4		0	0.0	
	Unknown	0		21			6		
Location	Head	4186	72.8	62	73.8	0.615	9	56.3	0.337
	Body	697	12.1	7	8.3		4	25.0	
	Tail	306	5.3	6	7.1		2	12.5	
	All segments of pancreas	24	0.4	1	1.2		0	0.0	
	Two segments of pancreas	537	9.3	8	9.5		1	6.3	
	Unknown	8		6			0		
TS	TS2	3921	68.1	65	72.2	0.404	12	75.0	0.554
	TS3	1837	31.9	25	27.8		4	25.0	
	Unknown	0		0			0		
T	Tis	0	0.0	0	0.0	<0.001	0	0.0	0.001
	T1	0	0.0	0	0.0		0	0.0	
	T2	239	4.4	26	29.4		0	0.0	
	T3	1434	26.5	52	58.4		11	68.8	
	T4	3742	69.1	11	12.2		5	31.3	
	Unknown	343		1			0		
N	N0	1629	30.9	46	51.1	<0.001	3	18.8	0.02
	N1	1251	23.8	33	36.7		9	56.3	
	N2	1160	22.0	10	11.1		3	18.8	
	N3	1225	23.3	1	1.1		1	6.3	
	Unknown	493		0			0		
M	M (−)	4177	72.8	88	97.8	<0.001	16	100	0.015
	M (+)	1560	27.2	2	2.2		0	0.0	
	Unknown	21		0			0		
Stage	0	0	0.0	0	0.0	<0.001	0	0.0	0.007
	I	0	0.0	0	0.0		0	0.0	
	II	113	2.2	25	27.8		0	0.0	
	III	925	18.0	41	45.6		7	43.8	
	IVA	1854	36.1	17	18.9		8	50.0	
	IVB	2244	43.7	6	6.7		1	6.3	
	Unknown	642		1			0		

P value compared with PDAC.

Clinicopathological Comparison of TS2 or TS3 PDAC and TS2 or TS3 PDAC Derived From IPMN and Concomitant With IPMN

Next, we compared the tumors that were TS2 (2.0 cm < tumor size ≤ 4.0 cm) or TS3 (4.0 cm < tumor size ≤ 6.0 cm) in size because TS2 and TS3 tumors were the most frequent sizes diagnosed in patients with PDAC, PDAC derived from IPMN, and PDAC concomitant with IPMN of this series. A total of 5578 patients had TS2 or TS3 PDAC, 90 patients had TS2 or TS3 PDAC derived from IPMN and 16 had TS2 or TS3 PDAC concomitant with IPMN (Table 7). These 3 groups of PDAC were compared to examine whether the type TS2 or TS3

TABLE 9. Median Survival of PDAC, PDAC Derived From IPMN, and PDAC Concomitant With IPMN (TS2 or TS3)

PDAC (n = 5578)		PDAC Derived From IPMN (n = 90)		PDAC Concomitant With IPMN (n = 16)		Results of the Log-Rank Test (*P*)	
n	MST, mo	n	MST, mo	n	MST, mo	PDAC vs PDAC Derived From IPMN	PDAC vs PDAC Concomitant With IPMN
5578	11	90	46	16	24	<0.001	0.002

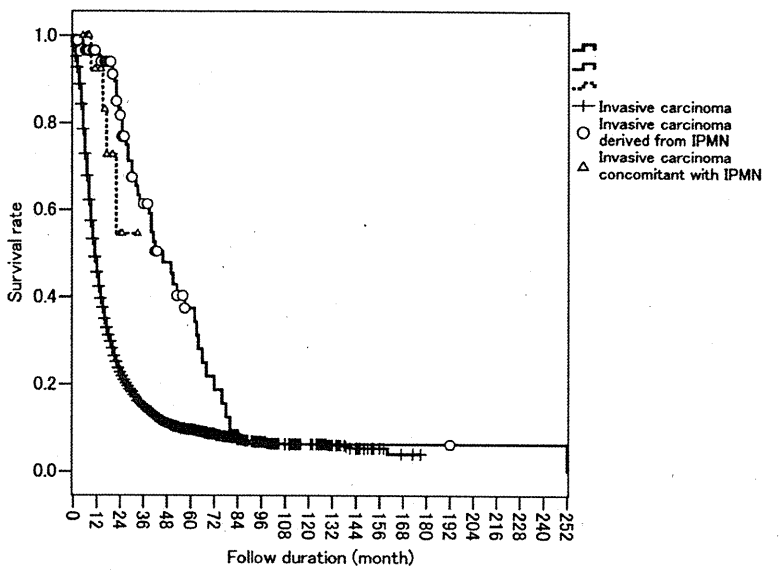

	Survival rate		
	1-year	3-year	5-year
PDAC	50%	16%	10%
PDAC derived from IPMN	96%	62%	38%
PDAC concomitant with IPMN	93%	60%	N.A.

*p<0.001 ** p=0.002

FIGURE 3. Survival curves of PDAC, PDAC derived from IPMN, and PDAC concomitant with IPMN (TS2 or TS3).

PDAC tumors were different from the TS2 or TS3 PDAC derived from IPMN or the TS2 or TS3 PDAC concomitant with IPMN. The T number in the TS2 or TS3 PDAC was significantly greater than for PDAC derived from IPMN and TS2 or TS3 PDAC concomitant with IPMN (Table 8). Lymph node and distant metastases were significantly more frequent and more extensive in TS2 or TS3 PDAC than in TS2 or TS3 PDAC derived from IPMN and TS2 or TS3 PDAC concomitant with IPMN. Distant metastasis was also more frequent in TS2 or TS3 PDAC than in TS2 or TS3 PDAC derived from IPMN and TS2 or TS3 PDAC concomitant with IPMN. The stages of TS2 or TS3 PDAC were more advanced than those of TS2 or TS3 PDAC derived from IPMN and TS2 or TS3 PDAC concomitant with IPMN.

The MST of patients with TS2 or TS3 PDAC was 11 months, being significantly shorter than the 46 months ($P < 0.001$) of the patients with TS2 or TS3 PDAC derived from IPMN and 24 months ($P = 0.002$) of those with TS2 or TS3 PDAC concomitant with IPMN (Table 9). The MSTs of PDAC derived from IPMN and concomitant with IPMN were longer than those of ordinary PDAC for each stage. The survival curves of patients with TS2 or TS3 PDAC were more unfavorable than those of TS2 or TS3 PDAC derived from IPMN ($P < 0.001$) and of TS2 or TS3 PDAC concomitant with IPMN ($P = 0.002$; Fig. 3). The 1-, 3-, and 5-year survival rates of ordinary TS2 or TS3 PDAC were 50%, 16%, and 10%, respectively, whereas those of TS2 or TS3 PDAC derived from IPMN were 96%, 62%, and 38%, respectively, and those of TS2 or TS3 PDAC concomitant IPMN were 93%, 60%, and NA (not available).

DISCUSSION

The definition of PDAC derived from IPMN and PDAC concomitant with IPMN was proposed in this study mainly with regard to the topological relationship between the 2 lesions and the presence or absence of a histological transition between the 2 conditions. This was a multi-institutional study, and we could not use *mucin profiles* and molecular biological examination for the differentiation. A total of 765 patients with IPMN were classified into 5 categories, that is, 381 (50%) with IPMA, 201 (26%) with IPMC (157 with noninvasive and 44 with minimally invasive disease), 122 (16%) with PDAC derived from IPMN, 31 (4%) with PDAC concomitant with IPMN, and 30 (4%) with PDAC of undetermined status with regard to IPMN. When the 2 groups composed of PDAC derived from IPMN and PDAC

TABLE 10. Pancreatic Ductal Adenocarcinoma, PDAC Derived From IPMN, and PDAC Concomitant With IPMN

	PDAC		PDAC Derived From IPMN		PDAC Concomitant With IPMN
Age, yr	64	<	67	≒	67
Sex, M/F	M: 60%	≒	M: 60%	≒	M: 60%
Site	H ≫ B, T		H ≫ B, T		H > B, T
Type (IPMN)			MPD Br		Br
Histological diagnosis	Tub		Muc (30%)		Tub
Tis	big	>	smaller	>	smallest
T	big	>	smaller	>	smallest
N (+)	70%	>	50%	≒	50%
M (+)	30%	>	3%	≒	0%
Stage	Advanced	>	Earlier	>	Earliest
MST, mo	12	<	46	≒	57

concomitant with IPMN were compared with ordinary PDAC, the mean ages of the 2 groups were higher than those of the non-IPMN PDAC group (Table 10). Mucinous carcinoma was more frequently seen in the group of PDAC derived from IPMN than in the other 2 groups. Pancreatic ductal adenocarcinoma concomitant with IPMN was more frequently located in the body or tail of the pancreas than were PDAC derived from IPMN and ordinary PDAC. Pancreatic ductal adenocarcinoma derived from IPMN and concomitant with IPMN were significantly smaller than ordinary PDAC in size and showed less invasive and extensive growth than ordinary PDAC. The median survivals of the 2 groups were significantly longer than that of patients with typical PDAC when compared overall and when limited to TS2 or TS3 cases.

Intraductal papillary mucinous neoplasm progresses from adenoma to carcinoma (noninvasive, then minimally invasive, and finally to PDAC derived from IPMN).[1–3,7,8] Yamaguchi et al[5] first reported PDAC concomitant with IPMN in 2002. Thereafter, this combination has been reported mainly in Japan,[9,10] and the development of pancreatic cancer apart from IPMN has been also reported during the follow-up of branch duct IPMN.[11,12] When IPMN and PDAC are present near each other, the distinction between PDAC derived from IPMN and PDAC concomitant with IPMN is difficult to make. There has been some confusion about the definition of the 2 conditions. In this series, we proposed diagnostic criteria of the 2 diseases based on the topological relationship and the presence or absence of a transitional area between the 2 diseases. In this series, we did not perform *mucin profiles* and molecular biological examinations because the present study was a multi-institutional analysis. If we added molecular biology to the criteria, we might have been able to differentiate the 2 conditions more precisely, decreasing the number of patients included in the "undetermined" group.

The reported incidence of PDAC concomitant with IPMN was 9%[5] or 4%[10] in 2 series of surgically resected IPMN. Ingkakul et al[13] reported that 22 (9.3%) of 236 patients with IPMN had concomitant PDAC synchronously or metachronously, and their multivariate analysis revealed that worsening of diabetes mellitus and an abnormal serum CA 19-9 level are 2 significant predictors of the presence of PDAC in IPMN. The development of independent PDAC has been reported in the follow-up of patients with IPMN.[11,12,14] Tada et al[11] reported that PDAC developed in 5% of patients with IPMN during a 3.8-year follow-up. Uehara et al[12] showed an 8% incidence of PDAC developing in 60 patients with branch duct IPMN during the mean follow-up period of 87 months. The 5-year rate of development of PDAC was 6.9%, and the incidence of PDAC was 1.1% per year. Tanno et al[14] showed that 4 (4.5%) of 89 patients with branch duct IPMN developed PDAC during a median follow-up of 64 months. When the new definition is applied, the incidence of PDAC concomitant with IPMN in the present series was 4.1%, which was lower than in the previous reports. This difference might come from the strict definition in this series and the multi-institutional collection of surgically resected cases.

Some have reported that the clinical outcome of patients with PDAC derived from IPMN is better than that for patients with ordinary PDAC because PDAC derived from IPMN is diagnosed at an earlier phase[15] or because the clinicopathological features of PDAC derived from IPMN are different from those of ordinary PDAC.[16–18] A global genomic analysis of IPMN showed significant molecular features that were different from ordinary PDAC.[19] In this series, the clinical outcome of patients with PDAC derived from IPMN was better than that of ordinary PDAC when compared overall and when limited to TS2 or TS3 tumors in size. Patients with IPMN related to PDAC (PDAC derived from IPMN and PDAC concomitant with IPMN) showed a longer MST than those with ordinary PDAC in each stage. Therefore, the biological behavior of PDAC derived from IPMN may be different from ordinary PDAC.

We first reported that the clinical outcome of patients with PDAC concomitant with IPMN was better than that of ordinary PDAC because PDAC concomitant with IPMN was detected at an earlier stage because of the presence of IPMN.[5] In this series, we compared the clinical course of PDAC concomitant with IPMN and that of ordinary PDAC when compared overall and when limited to TS2 or TS3 tumors in size. The clinical course of PDAC concomitant with IPMN was better than ordinary PDAC. Thus, the biological behavior of PDAC concomitant with IPMN may also be different from that of ordinary PDAC.

Concerning pancreatic carcinogenesis, 2 main pathways have been considered: (1) from PanIN to PDAC[20–22] and (2) from IPMN to mucinous carcinoma.[23,24] Others have reported that mucinous carcinoma of the pancreas often originates from IPMN.[23,24] In the present series, mucinous carcinoma was more frequently present in PDAC derived from IPMN than PDAC alone or PDAC concomitant with IPMN. In minimally invasive foci of IPMC, IPMC invaded the stroma in the form of mucinous carcinoma in about a half of the patients.[3] With regard to the histological type, approximately one-third of the PDAC derived from IPMN (41/122) was mucinous carcinoma, although most of PDAC concomitant with IPMN (28/31) was tubular adenocarcinoma, which is similar to ordinary PDAC. These facts may support the hypothesis that most of the mucinous carcinoma of the pancreas originates from IPMC.

This series is a collective series of surgically resected IPMN, PDAC derived from IPMN, and PDAC concomitant with IPMN, and there are some biases that resulted from this limitation. In this series, the PDAC derived from IPMN or concomitant with IPMN were less invasive and showed less extensive growth than those of ordinary PDAC. The overall survival rates of PDAC derived from IPMN and PDAC concomitant with IPMN were significantly better than those of ordinary PDAC. Even when limited to TS2 or TS3 tumors, PDAC derived from IPMN and PDAC concomitant with IPMN showed less aggressive growth than TS2 or TS3 PDAC. Therefore, PDAC derived from IPMN and concomitant with IPMN may have more favorable biological features than ordinary PDAC. Further examination of the natural history of PDAC derived from IPMN and concomitant with IPMN is therefore necessary before any definitive conclusions can be made about the origins, behavior, and lethality of the different types of pancreatic cancer.

REFERENCES

1. Solcia E, Capella C, Kloeppel G. *Tumors of the Pancreas, Third series, Fascicle 20.* Washington, DC: Armed Forces Institutes of Pathology; 1995.
2. Kloeppel GSE, Longnecker DS, Capella C, et al. *World Health Organization International Histological Classification of Tumours Histological Typing of Tumours of Exocrine Pancreas.* 2nd ed. Berlin, Germany: Springer-Verlag; 1996.
3. Yamaguchi K, Tanaka M. *Atlas of Cystic Neoplasms of the Pancreas.* Fukuoka, Japan: Kyushu University Press/KARGER; 2000.
4. Yamaguchi K, Nakamura K, Yokohata K, et al. Pancreatic cyst as a sentinel of in situ carcinoma of the pancreas. Report of two cases. *Int J Pancreatol.* 1997;22(3):227–231.
5. Yamaguchi K, Ohuchida J, Ohtsuka T, et al. Intraductal papillary-mucinous tumor of the pancreas concomitant with ductal carcinoma of the pancreas. *Pancreatology.* 2002;2(5):484–490.
6. Japan Pancreas Society. *Classification of Pancreatic Carcinoma.* 2nd English ed. Tokyo, Japan: Kanehara & Co, Ltd.; 2003.

7. Hamilton S, Aaltonen L. *World Health Organization Classification of Tumours Pathology & Genetics Tumours of the Digestive System.* Lyon, France: IARC Press; 2000.
8. Hruban R, Pitman M, Klimstra D. *AFIP Atlas of Tumor Pathology Series 4 Fascicle 6 Tumors of the Pancreas.* Washington, DC: American Registry of Pathology and Armed Forces Institute of Pathology; 2007.
9. Nakaizumi A, Tanaka S, Oshikawa O, et al. Branch duct type IPMN concomitant with usual invasive ductal carcinoma. *Tan to Sui.* 2002;23(12):1013–1019.
10. Kamisawa T, Tu Y, Egawa N, et al. Malignancies associated with intraductal papillary mucinous neoplasm of the pancreas. *World J Gastroenterol.* 2005;11(36):5688–5690.
11. Tada M, Kawabe T, Arizumi M, et al. Pancreatic cancer in patients with pancreatic cystic lesions: a prospective study in 197 patients. *Clin Gastroenterol Hepatol.* 2006;4(10):1265–1270.
12. Uehara H, Nakaizumi A, Ishikawa O, et al. Development of ductal carcinoma of the pancreas during follow-up of branch duct intraductal papillary mucinous neoplasm of the pancreas. *Gut.* 2008;57(11):1561–1565.
13. Ingkakul T, Sadakari Y, Ienaga J, et al. Predictors of the presence of concomitant invasive ductal carcinoma in intraductal papillary mucinous neoplasm of the pancreas. *Ann Surg.* 2010;251(1):70–75.
14. Tanno S, Nakano Y, Koizumi K, et al. Pancreatic ductal adenocarcinomas in long-term follow-up patients with branch duct intraductal papillary mucinous neoplasms. *Pancreas.* 2010;39(1):36–40.
15. Poultsides GA, Reddy S, Cameron JL, et al. Histopathologic basis for the favorable survival after resection of intraductal papillary mucinous neoplasm–associated invasive adenocarcinoma of the pancreas. *Ann Surg.* 2010;251(3):470–476.
16. Fukushima N, Mukai K, Sakamoto M, et al. Invasive carcinoma derived from intraductal papillary-mucinous carcinoma of the pancreas: clinicopathologic and immunohistochemical study of eight cases. *Virchows Arch.* 2001;439(1):6–13.
17. Iacobuzio-Donahue CA, Klimstra DS, Adsay NV, et al. Dpc-4 protein is expressed in virtually all human intraductal papillary mucinous neoplasms of the pancreas: comparison with conventional ductal adenocarcinomas. *Am J Pathol.* 2000;157(3):755–761.
18. Murakami Y, Uemura K, Sudo T, et al. Invasive intraductal papillary-mucinous neoplasm of the pancreas: comparison with pancreatic ductal adenocarcinoma. *J Surg Oncol.* 2009;100(1):13–18.
19. Fritz S, Fernandez-del Castillo C, Mino-Kenudson M, et al. Global genomic analysis of intraductal papillary mucinous neoplasms of the pancreas reveals significant molecular differences compared to ductal adenocarcinoma. *Ann Surg.* 2009;249(3):440–447.
20. Hruban RH, Adsay NV, Albores-Saavedra J, et al. Pancreatic intraepithelial neoplasia: a new nomenclature and classification system for pancreatic duct lesions. *Am J Surg Pathol.* 2001;25(5):579–586.
21. Longnecker DS, Adsay NV, Fernandez-del Castillo C, et al. Histopathological diagnosis of pancreatic intraepithelial neoplasia and intraductal papillary-mucinous neoplasms: interobserver agreement. *Pancreas.* 2005;31(4):344–349.
22. Sipos B, Frank S, Gress T, et al. Pancreatic intraepithelial neoplasia revisited and updated. *Pancreatology.* 2009;9(1–2):45–54.
23. Seidel G, Zahurak M, Iacobuzio-Donahue C, et al. Almost all infiltrating colloid carcinomas of the pancreas and periampullary region arise from in situ papillary neoplasms: a study of 39 cases. *Am J Surg Pathol.* 2002;26(1):56–63.
24. Liszka L, Zielinska-Pajak E, Pajak J, et al. Colloid carcinoma of the pancreas: review of selected pathological and clinical aspects. *Pathology.* 2008;40(7):655–663.

High *EGFR* mRNA expression is a prognostic factor for reduced survival in pancreatic cancer after gemcitabine-based adjuvant chemotherapy

HAYATO FUJITA[1], KENOKI OHUCHIDA[1,2], KAZUHIRO MIZUMOTO[1,3], SOICHI ITABA[4], TETSUHIDE ITO[4], KOHEI NAKATA[1,5], JUN YU[1], TADASHI KAYASHIMA[1], AKIFUMI HAYASHI[1,5], RYOTA SOUZAKI[6], TATSURO TAJIRI[6], MANABU ONIMARU[1], TATSUYA MANABE[1], TAKAO OHTSUKA[1] and MASAO TANAKA[1]

Departments of [1]Surgery and Oncology, and [2]Advanced Medical Initiatives, Graduate School of Medical Sciences, Kyushu University; [3]Kyushu University Hospital Cancer Center, 3-1-1 Maidashi; Departments of [4]Medicine and Bioregulatory Science, [5]Anatomic Pathology, and [6]Pediatric Surgery, Graduate School of Medical Sciences, Kyushu University, 3-1-1 Maidashi, Fukuoka 812-8582, Japan

Received October 26, 2010; Accepted December 20, 2010

DOI: 10.3892/ijo.2011.908

Abstract. Pancreatic ductal adenocarcinoma (PDAC) still presents a major therapeutic challenge and a phase III clinical trial has revealed that the combination of gemcitabine and a human epidermal growth factor receptor type I (HER1/EGFR) targeting agent presented a significant benefit compared to treatment with gemcitabine alone. The aim of this study was to investigate *EGFR* mRNA expression in resected PDAC tissues and its correlation with patient prognosis. We obtained formalin-fixed paraffin-embedded (FFPE) tissue samples from 88 patients with PDAC who underwent pancreatectomy, and measured *EGFR* mRNA levels by quantitative real-time reverse transcription-polymerase chain reaction. The high-level *EGFR* group had significantly shorter disease-free-survival (p=0.029) and overall-survival (p=0.014) as shown by univariate analyses, although these did not reach statistical significance, as shown by multivariate analyses. However, we found that high *EGFR* expression was an independent prognostic factor in patients receiving gemcitabine-based adjuvant chemotherapy (p=0.023). Furthermore, we measured *EGFR* mRNA levels in 20 endoscopic ultrasound-guided fine needle aspiration (EUS-FNA) cytological specimens. Altered *EGFR* levels were distinguishable in microdissected neoplastic cells from EUS-FNA cytological specimens compared to those in whole cell pellets. In conclusion, quantitative analysis of *EGFR* mRNA expression using FFPE tissue samples and microdissected neoplastic cells from EUS-FNA cytological specimens could be useful in predicting prognosis and sensitivity to gemcitabine in PDAC patients.

Correspondence to: Dr Kenoki Ohuchida or Dr Kazuhiro Mizumoto, Department of Surgery and Oncology, Graduate School of Medical Sciences, Kyushu University, 3-1-1 Maidashi, Fukuoka 812-8582, Japan
E-mail: kenoki@med.kyushu-u.ac.jp
E-mail: mizumoto@med.kyushu-u.ac.jp

Key words: epidermal growth factor receptor, pancreatic cancer, reverse transcription-polymerase chain reaction, formalin-fixed paraffin-embedded samples, endoscopic ultrasound-guided fine needle aspiration

Introduction

Pancreatic ductal adenocarcinoma (PDAC) is one of the most lethal and aggressive human malignancies, and it is the fourth leading cause of tumor-related deaths in the industrialized world (1,2). The vast majority of patients with PDAC have poor outcomes due to the aggressive nature of the tumor and difficulties in early diagnosis due to the lack of early disease-specific signs and symptoms. Only 10-20% of patients with PDAC have a chance of curative resection (3) and, even if the curative resection is performed, the post-operative 5-year survival rate is only 15-25% due to a high recurrence rate (4,5). Two randomized clinical phase III trials of adjuvant chemotherapy (AC) for PDAC have shown significant increases in overall survival (OS) and disease-free survival (DFS). However, their efficacy was limited and insufficient (6,7). To improve the prognosis of patients with PDAC, individualized chemotherapy based on the gene expression profiles of the individual's own cancer tissues, could be a potent strategy.

Human epidermal growth factor receptor type 1 (HER1/EGFR) is a receptor tyrosine kinase. Binding of ligand growth factors, such as epidermal growth factor (EGF) and transforming growth factor (TGF)-α to EGFR leads to receptor phosphorylation and activation of downstream Ras/mitogen-activated protein kinase (MAPK) signaling, thereby enhancing the malignant behavior of cancer cells (8,9). There is increasing

evidence showing that the dysregulation of EGFR pathways by overexpression or constitutive activation can promote tumor growth and metastasis, and that this is associated with poor prognosis and tumor aggressiveness in many human malignancies, including pancreatic cancer (10-13). To improve the prognosis of PDAC patients, the blockade of the EGFR signaling pathway could be a potent strategy (9,14). The EGFR signaling blockade has been reported to decrease growth and metastasis in an orthotopic implantation murine model of pancreatic cancer cells (15) and to improve the efficacy of gemcitabine in human pancreatic tumor xenograft models (16).

At the time of diagnosis, >80% of PDAC patients present with either locally advanced or metastatic disease (3). Therefore, patients with unresectable advanced PDAC require cytopathological assessment using endoscopic ultrasound-guided fine needle aspiration (EUS-FNA) or pancreatic juice specimens to predict their sensitivity to chemotherapeutic agents and prognosis. Quantitative mRNA analysis of genes associated with sensitivity to chemotherapeutic agents, or with patient prognosis could be suitable for clinical use as this method enables us to reproducibly detect gene expression, even with small samples (17). In the current study, we investigated the correlation between *EGFR* expression and the prognosis of patients with PDAC. To elucidate the role of *EGFR* expression in gemcitabine sensitivity, we also investigated the association between receptor expression levels and treatment outcomes in PDAC patients receiving gemcitabine-based AC. Furthermore, we quantified *EGFR* expression in cytological specimens obtained by EUS-FNA to examine the possible utility of such samples for quantifying the mRNA levels of these predictive factors.

Materials and methods

Patients and pancreatic tissues. Our study subjects comprised of 88 patients who underwent pancreatectomy for PDAC at the Department of Surgery and Oncology, Kyushu University Hospital (Fukuoka, Japan) from 1992 to 2007. The patients (54 male and 34 female) had a median age of 65 years (range, 36-86 years). Eighteen of the 88 patients received no AC (non-AC group). Thirty-six of the 88 patients received gemcitabine-based AC (GEM group), consisting of two or more cycles of 1,000 mg/m^2/d gemcitabine on days 1, 8 and 15 every 28 days, and three or more cycles of 1,000 mg/m^2/d gemcitabine on days 1 and 8 every 21 days. Nineteen of the 88 patients received other forms of AC (other AC group), including 5 patients orally administered S-1 (80-100 mg/body), 7 patients orally administered tegafur (400-800 mg/body), and 7 patients treated with a bolus of 5-fluorouracil (250-500 mg/body). The remaining 15 patients did not receive adequate AC due to their poor performance status. We recommended that patients had follow-up visits every 3 months for 2 years, then visits every 6 months for 3 years, and then annual visits. DFS was defined as the time from the date of pancreatic resection to the date of local or distant recurrence. The date of recurrence was defined as the date of the first subjective symptom heralding relapse, or the date of documentation of recurrent disease, independent of site, as assessed by diagnostic imaging techniques (whichever occurred first). Data for patients without recurrence were censored at the time of the last follow-up visit. OS was measured from the date of pancreatic resection to the date of death. Fifty-eight patients died during follow-up and the other patients were censored at the time of the last follow-up visit. Data were analyzed in December 2009 and follow-up data from all cases were available. The median observation time for DFS was 9 months (range, 0.5-114 months) and OS was 18 months (range, 0.5-114 months). The clinicopathological characteristics of the tumors collected from 88 patients are provided in Table I. Additionally,

Table I. Clinicopathological characteristics of the patients (n=88).

Median age	65 years (range, 36–86 years)
Gender (male/female)	54 (61.4%)/34 (38.6%)
Histological diagnosis	
Adenocarcinoma	86 (97.7%)
Adenosquamous carcinoma	2 (2.3%)
Adjuvant chemotherapy (AC)	
No	18 (20.5%)
Yes	55 (62.5%)
Gemcitabine-based AC	36 (40.9%)
Other AC	19 (21.6%)
Radiotherapy including IOR	
Yes	23 (26.1%)
No	53 (60.2%)
pT category	
pT1	5 (5.8%)
pT2	3 (3.4%)
pT3	78 (89.7%)
pT4	1 (1.1%)
pN category	
pN0	27 (31.0%)
pN1	60 (69.0%)
UICC stage	
I	6 (6.9%)
II	78 (89.7%)
III	1 (1.1%)
IV	2 (2.3%)
Histological grade	
G1	20 (23.3%)
G2	33 (38.4%)
G3	33 (38.4%)
Residual tumor category	
R0	55 (63.9%)
R1	31 (36.1%)
Vessel invasion	
Positive	55 (63.2%)
Negative	32 (36.8%)
Neural invasion	
Positive	72 (82.8%)
Negative	15 (17.2%)

in order to compare the *EGFR* expression levels in PDAC tissues to those in non-malignant pancreatic specimens, a total of 40 non-malignant pancreatic tissues, including 10 normal pancreatic tissues resected with bile duct carcinoma and 30 chronic pancreatitis tissues, were also obtained.

All resected specimens were fixed in formalin and embedded in paraffin, and all tissues adjacent to the specimens were evaluated histologically according to the criteria of the World Health Organization. Two pathologists were in agreement as regards the pathological features of all cases and the diagnoses were confirmed. The tumor stage was assessed according to the Union Internationale Contre le Cancer (UICC) and the American Joint Committee on Cancer guidelines (18). The study was approved by the Ethics Committee of Kyushu University and conducted according to the Ethical Guidelines for Human Genome/Gene Research enacted by the Japanese Government and the Helsinki Declaration.

Immunohistochemistry. A total of 25 sections (4-μm thick) from formalin-fixed paraffin-embedded (FFPE) specimens from 88 patients with PDAC and 15 sections from 40 non-malignant cases, including seven sections from normal pancreas resected with bile duct carcinoma, and 8 sections from chronic pancreatitis patients, were deparaffinized in xylene and hydrated in graded ethanol. Endogenous peroxidase activity was blocked by incubation with 3% hydrogen peroxide in methanol for 30 min. Antigen retrieval was achieved by autoclaving the sections in citrate buffer at pH 6.0. The Histofine SAB-PO(R) kit (Nichirei, Tokyo, Japan) was used for immunohistochemical labeling. The sections were incubated with 1.5% normal goat serum/phosphate-buffered saline, followed by incubation with a rabbit polyclonal anti-EGFR antibody (Santa Cruz Biotechnology, Santa Cruz, CA) at a 1:50 dilution overnight at 4˚C. The sections were incubated with biotinylated anti-rabbit immunoglobulin solution for 20 min followed by peroxidase-labeled streptavidin for 20 min. Immunocomplexes were visualized using stable 3,3'-diaminobenzidine tetrahydrochloride (Dojin, Kumamoto, Japan). The sections were rinsed with distilled water and counterstained with hematoxylin for 10 sec. The amount of EGFR immunoreactivity was evaluated using the following scale according to the percentage of EGFR-positive cancer cells: 0, <5%; 1, 5–25%; 2, 26–50%; and 3, >51%. Staining intensity was scored semi-quantitatively as follows: 0, absent; 1, weak; 2, moderate; 3, strong. To perform the quantitative analysis of EGFR immunoreactivity, the following combined score was determined: Degree of staining = quantity x intensity. We also performed additional staining without primary antibodies as the negative control. All slides were evaluated independently by three investigators (H.F., A.H. and K.N.) without any knowledge of the background of each case.

Cytological specimens. Cytological specimens were obtained at the time of cytological examination and diagnosis from the pathological laboratory of Kyushu University Hospital. In brief, cytological specimens were divided into whole cell pellets (WCP) and into three or more smears as soon as possible after retrieval. Smears were processed in three different ways as described previously (17). Two smears were mounted on standard glass slides for Hemacolor staining (Merck KGaA, Darmstadt, Germany) and Papanicolaou staining, then used for rapid cytological diagnosis and strict cytological diagnosis, respectively. These two smears were examined histologically by cytopathologists and diagnosis was confirmed according to the Papanicolaou Classification. The third smear of each specimen was mounted on membrane slides (Leica Microsystems, Wetzlar, Germany) for laser capture microdissection (LCM). These smears were stained in 1% toluidine blue staining solution or by Hemacolor staining. Twenty cytological specimens were obtained from patients at the Kyushu University Hospital who underwent EUS-FNA cytology and who were cytopathologically diagnosed with PDAC.

Isolation of RNA. Total RNA was isolated from FFPE tissue samples using the RNeasy FFPE kit (Qiagen, Tokyo, Japan) with some modification to the manufacturer's instructions after macrodissection based on a review of representative hematoxylin and eosin-stained slides as described previously (19). Total RNA was extracted from cells isolated by micro-dissection according to the standard acid guanidinium thiocyanate-phenol-chloroform protocol (20), with or without glycogen (Funakoshi, Tokyo, Japan).

Quantitative real-time reverse transcription-polymerase chain reaction (qRT-PCR). qRT-PCR was performed using the Chromo4 Real-Time PCR Detection System (Bio-Rad Laboratories, Hercules, CA, USA) and the LightCycler 480 II Real-Time PCR System (Roche Diagnostics) for 40 cycles of 15 sec at 95˚C and 1 min at 55˚C with the QuantiTect SYBR-Green Reverse Transcription-PCR kit (Qiagen) in accordance with the manufacturer's instructions (21). We designed specific primers for *EGFR* (forward primer, 5'-cctatgtgcagaggaa ttatgatcttt-3'; and reverse primer, 5'-ccactgtgttgagggcaatg-3') and *β-actin* (forward primer, 5'-tgagcgcggctacagctt-3'; and reverse primer, 5'-tccttaatgtcacgcacgattt-3'), and screened a database using BLASTN to confirm the primer specificities. The level of each mRNA was calculated from a standard curve constructed using total RNA from Capan-1, a human pancreatic cancer cell line. The level of *EGFR* mRNA was normalized to that of *β-actin*. The PCR product sizes of *EGFR* and *β-actin* primers were small [88 base pairs (bp) and 59 bp, respectively], which allowed for accurate and sensitive qRT-PCR analysis despite the fragmented RNA extracted from the FFPE tissue specimens (22,23).

Statistical analyses. Statistical analyses and graphical presentations were performed using JMP 7.01 software (SAS Institute, Cary, NC, USA). Values were expressed as the means ± SD. Data were analyzed using the Kruskal-Wallis test if comparisons involved three groups, and the Mann-Whitney U-test and Spearman's rank-correlation test if comparisons involved two groups as normal distributions were not obtained. *EGFR* expression was split into high- and low-level groups using recursive descent partition analysis, as described by Hoffmann *et al* (24). Categorical variables were compared using the χ^2 test (Fisher's exact probability test). Survival curves were constructed using the Kaplan-Meier product-limit method and were compared using the log-rank test. To evaluate independent prognostic factors associated with survival, multivariate Cox

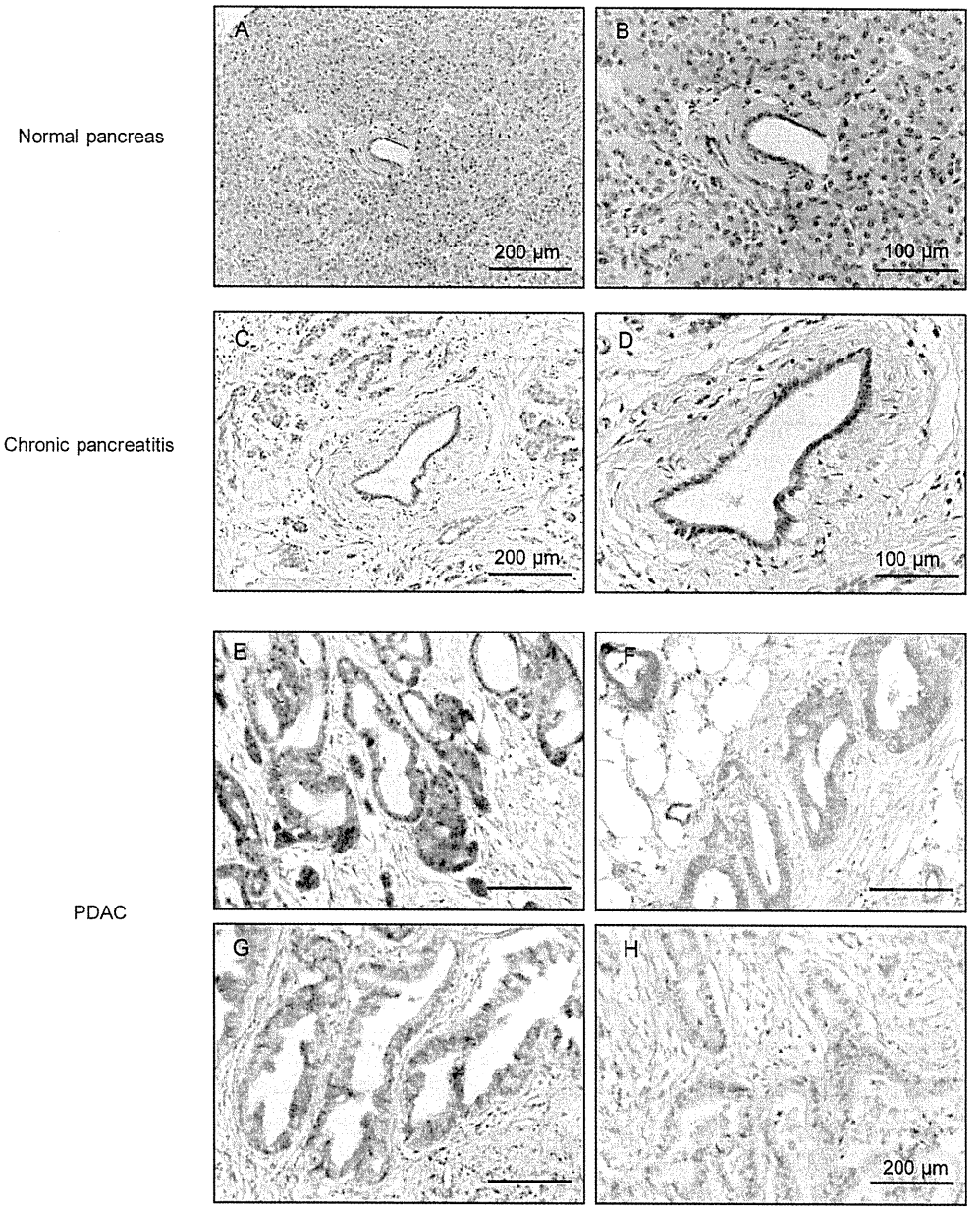

Figure 1. Immunohistochemical analysis of EGFR in normal pancreas, chronic pancreatitis and PDAC tissues. Weak to moderate immunoreactivity for EGFR was detected in some acinar cells and pancreatic ductal cells (A-D). In PDAC tissues, immunoreactivity for EGFR was observed on the surface and in the cytoplasm of cancer cells (E-G), with no immunoreactivity in the surrounding stroma (E-H). The immunoreactivity was different in respective cases (E, strong; F, moderate; G, weak expression; H, absent). Scale bars represent 200 μm (A, C, E-H) and 100 μm (B and D).

proportional hazards regression analysis was used. Statistical significance was defined as a p-value of <0.05.

Results

EGFR protein expression was correlated with EGFR mRNA expression. We performed immunohistochemical analyses on 15 sections of non-malignant pancreatic tissues, including 7 normal, 8 chronic pancreatitis tissues and 25 PDAC tissues. In agreement with the findings of previous studies (10,13), weak to moderate immunoreactivity for EGFR was detected in some acinar cells and pancreatic ductal cells (Fig. 1A-D). EGFR immunoreactivity was observed on the surface and in the cytoplasm of cancer cells within PDAC tissues, but none was observed in the surrounding stroma (Fig. 1E-G) (10,13). To investigate the correlation between EGFR immunoreactivity and *EGFR* mRNA expression levels within each FFPE tissue sample from resected PDAC tissue, we evaluated the degree of staining (quantity x intensity) for an anti-EGFR antibody, as the immunoreactivity was different in respective cases (Fig. 1E, strong; F, moderate; G, weak expression; and H, absent). We found a significant correlation between the degree of staining and *EGFR* mRNA expression levels [Fig. 2A; Spearman's rank-correlation coefficient (ϱ): 0.729, $p<0.0001$], and cases with a higher degree of immunoreactivity expressed significantly higher levels of *EGFR* mRNA compared with those with a lower degree of immunoreactivity (Fig. 2B; $p=0.0005$). These observations suggest that quantitative mRNA analysis of *EGFR* in macrodissected PDAC tissues may reflect *EGFR* protein expression levels in EGFR-

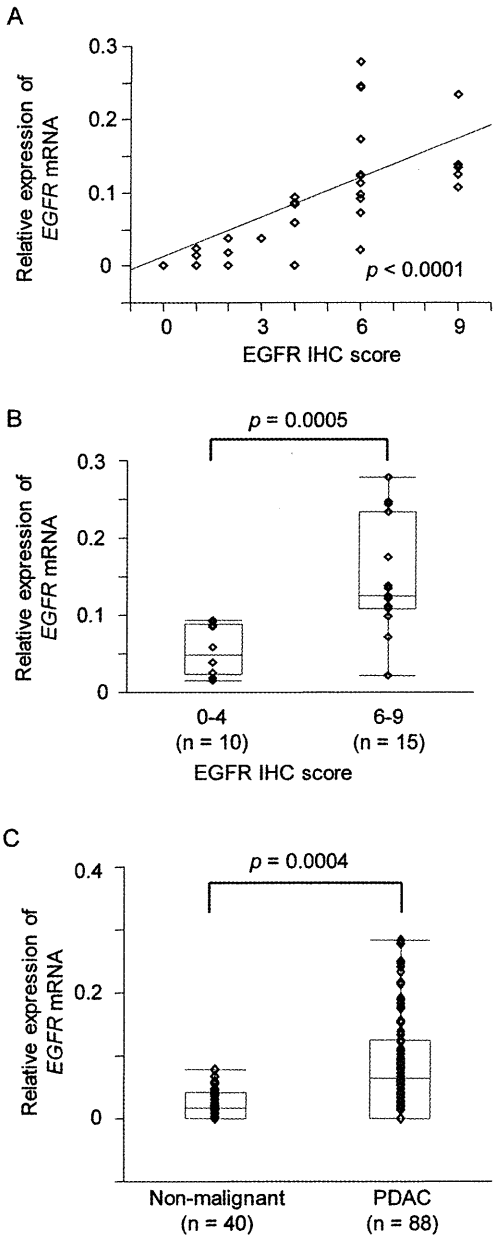

Figure 2. Correlation between EGFR immunoreactivity and *EGFR* mRNA expression levels in each FFPE tissue sample from resected PDAC tissues (A; n=25). We observed a significant correlation between the degree of staining (quantity x intensity) and *EGFR* mRNA expression levels [A; Spearman's rank-correlation coefficient (ϱ): 0.729, p<0.0001], and cases with a higher degree of staining (6-9; n=15) expressed significantly higher levels of *EGFR* mRNA compared to cases with a lower degree of staining (0-4; n=10) (B; p=0.0005). We found that *EGFR* expression levels in the PDAC samples (n=88) were significantly higher than those in the non-malignant samples (n=40) (C; p=0.0004).

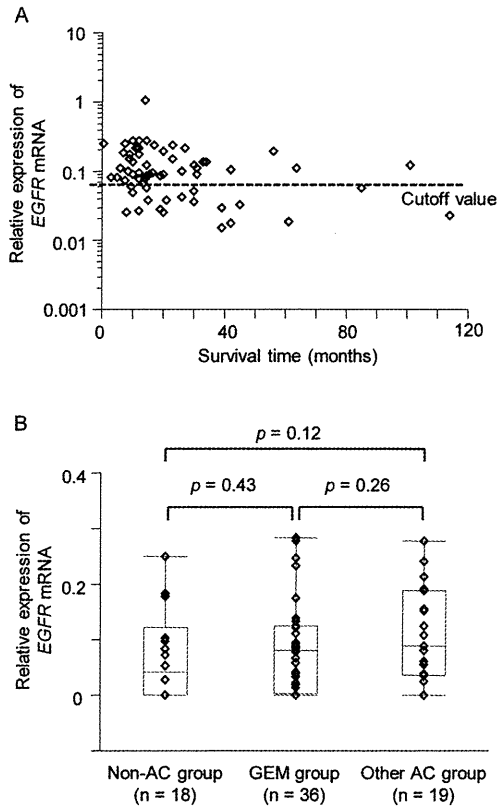

Figure 3. Quantitative analysis of *EGFR* mRNA expression levels in FFPE tissue samples from resected PDAC tissues (n=88) using qRT-PCR. After normalization to *β-actin* expression, we obtained 2 groups with high *EGFR* expression and low *EGFR* expression using a cut-off value (0.058) determined with recursive descent partition analysis, respectively (A). There was no significant difference in *EGFR* mRNA levels between the respective groups (non-AC group, n=18; GEM group, n=36; other AC group, n=19; p=0.26) (B).

expressing cancer cells. Additionally, although there was immunoreactivity for EGFR in some acinar and ductal cells in non-malignant cases, we found that *EGFR* expression levels in PDAC samples (n=88) were significantly higher than those in non-malignant samples (n=40) (Fig. 2C; p=0.0004).

Univariate and multivariate analyses of EGFR mRNA expression and survival time. We quantified *EGFR* mRNA expression levels in FFPE tissue samples from resected PDAC tissues using qRT-PCR. After normalization to *β-actin*, we obtained two groups (high *EGFR* expression and low *EGFR* expression) using a cut-off value (0.058) determined by recursive descent partition analysis of all patients (n=88) (Fig. 3A) (24). The high and low *EGFR* expression groups comprised of 46 and 42 cases, respectively. The relationship between *EGFR* mRNA expression and the clinicopathological factors seen in PDAC patients is shown in Table II. We found no significant correlation between *EGFR* mRNA expression and clinicopathological factors. In addition, there was no significant difference in *EGFR* mRNA levels between the non-AC group, the GEM group, and the other AC group (p=0.26; Fig. 3B).

Initially, we examined the independent markers that indicated poor prognosis in the 88 PDAC patients. Univariate analyses for DFS and OS (Table III) showed that conventional prognostic markers, such as pN status (p=0.0009 and p=0.0026, respectively), residual tumor category (R factor) (p<0.0001 and p<0.0001, respectively), and positive vessel invasion (p=0.0018 and p=0.0035, respectively) reached statistical significance, whereas the effect of AC did not (p=0.23 and p=0.066, respectively). High *EGFR* levels after normalization to *β-actin* were associated with a shorter DFS and OS (Table III and Fig. 4A-B; p=0.029 and p=0.014, respectively). Multivariate analysis based on the Cox proportional hazards model was performed on all parameters that were found to be significant by univariate analyses for DFS (Table IV) and OS

Table II. Relationship between *EGFR* mRNA expression and various clinicopathological factors.

Characteristics	*EGFR* mRNA expression[a]		P-value
	High-level group (n=46)	Low-level group (n=42)	
Age			0.808
≥65 years	24 (52.2%)	23 (54.8%)	
<65 years	22 (47.8%)	19 (45.2%)	
Adjuvant chemotherapy (AC)			0.484
No	8 (17.4%)	10 (23.8%)	
Yes	33 (71.7%)	22 (52.4%)	
Gemcitabine-based AC	21 (45.7%)	15 (35.7%)	
Other AC	12 (26.1%)	7 (16.7%)	
Radiotherapy			0.368
Yes	10 (21.7%)	13 (30.9%)	
No	29 (63.0%)	24 (57.1%)	
pT category			0.543
pT1/pT2	5 (10.9%)	3 (7.1%)	
pT3/pT4	41 (89.1%)	39 (92.9%)	
pN category			0.169
pN0	11 (23.9%)	16 (38.1%)	
pN1	34 (73.9%)	26 (61.9%)	
UICC stage			0.804
I	3 (6.5%)	3 (7.1%)	
II	41 (89.1%)	37 (88.1%)	
III/IV	1 (2.2%)	2 (4.8%)	
Histological grade			0.220
G1	10 (21.7%)	10 (23.8%)	
G2	14 (30.4%)	19 (45.2%)	
G3	21 (45.7%)	12 (28.6%)	
Residual tumor category			0.336
R0	26 (56.5%)	29 (69.0%)	
R1	18 (39.1%)	13 (30.9%)	
Vessel invasion			0.256
Positive	31 (67.4%)	24 (57.1%)	
Negative	14 (30.4%)	18 (42.9%)	
Neural invasion			0.891
Positive	37 (80.4%)	35 (83.3%)	
Negative	8 (17.4%)	7 (16.7%)	

[a]Cut-off value (0.058) was determined by recursive descent partition analysis of all patients (n=88).

(Table V). DFS was significantly dependent on the R factor (p<0.0001) and vessel invasion (p=0.038), whereas OS was significantly dependent on the R factor alone (p<0.0001). The effect of high *EGFR* levels did not reach statistical significance for either DFS or OS.

In order to determine which parameters were predictive for gemcitabine sensitivity, we then evaluated the correlation between each parameter and DFS in the GEM and non-AC groups. We found no significant correlation between the level of *EGFR* mRNA expression and clinicopathological factors in the GEM group (Table VI). Univariate survival analyses of the GEM group showed that pN status (p=0.0094), residual tumor (p=0.0004), and high *EGFR* level normalized to *β-actin* (Fig. 5A; p=0.068) reached statistical significance for DFS (Table VII). However, there was no significant correlation between the *EGFR* expression level and DFS in the non-AC group (p=0.30, Fig. 5C), although the number of patients who did not receive AC was limited. Multivariate analysis of the GEM group (Table VIII) showed that DFS was significantly dependent on both the R factor (p=0.0071) and high *EGFR* levels (p=0.010).

Similarly, we evaluated the correlation between each parameter and OS in the GEM and non-AC groups. Univariate survival analyses of the GEM group showed that the conventional prognostic markers, pN status (p=0.020), R factor (p=0.013), and high *EGFR* levels normalized to *β-actin* (Fig. 5B; p=0.054) reached statistical significance for OS (Table VII). However, the effect of *EGFR* expression levels

Table III. Univariate survival analysis of conventional prognostic factors and *EGFR* mRNA expression (n=88).

Characteristics	Number of cases	Median DFS (months)	P-value	Median OS (months)	P-value	5-year survival rate
EGFR mRNA expression[a]			0.029[b]		0.014[b]	
High	42	7.0		14.6		19.9%
Low	46	25.0		35.5		37.9%
Age			0.96		0.93	
≥65 years	47	12.0		26.0		24.6%
<65 years	41	8.0		19.0		35.4%
Adjuvant chemotherapy (AC)			0.23		0.066	
Yes	64	12.0		23.0		33.4%
No	20	7.0		12.1		14.3%
Radiotherapy			0.77		0.58	
Yes	23	12.0		23.0		29.5%
No	53	10.0		20.0		22.4%
pT category			0.34		0.54	
pT1/pT2	8	22.0		63.0		62.5%
pT3/pT4	80	8.0		23.0		25.5%
pN category			0.0009[b]		0.0026[b]	
pN0	27	36.0		45.0		49.3%
pN1	60	8.0		16.3		19.0%
UICC stage			0.14		0.28	
I	6	26.5		63.0		83.3%
II	78	8.0		20.9		25.3%
III/IV	3	16.0		19.8		0%
Histological grade			0.072		0.16	
G1/G2	54	14.0		30.0		31.9%
G3	33	8.0		14.6		27.4%
Residual tumor category			<0.001[b]		<0.001[b]	
R0	55	26.0		43.0		43.4%
R1	31	5.0		12.0		5.3%
Vessel invasion			0.0018[b]		0.0035[b]	
Positive	55	7.0		16.9		18.7%
Negative	32	31.0		45.0		45.0%
Neural invasion			0.95		0.76	
Positive	72	10.0		23.0		26.0%
Negative	15	14.0		19.0		24.3%

[a]Cut-off value (0.058) was determined by recursive descent partition analysis of all patients (n=88); [b]p<0.05.

Table IV. Multivariate DFS analysis (Cox regression model) of conventional prognostic factors and *EGFR* mRNA.

Characteristics	Relative risk	95% Confidence interval	P-value
High *EGFR* levels[a]	1.208	0.680-2.192	0.523
pN category (pN1)	1.939	0.966-4.166	0.063
Residual tumor category (pR1)	4.957	2.647-9.281	<0.0001[b]
Positive vessel invasion	1.942	1.036-3.825	0.038[b]

[a]Cut-off value (0.058) was determined by recursive descent partition analysis of all patients (n=88); [b]p<0.05.

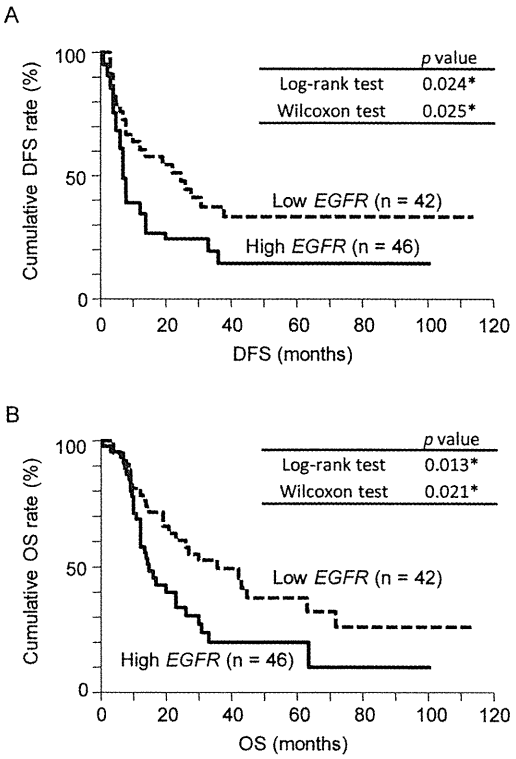

Figure 4. DFS and OS after resection of PDAC with high versus low *EGFR* expression. High *EGFR* mRNA levels were associated with a shorter DFS (A, p=0.029) and a shorter OS (B, p=0.014). *p<0.05.

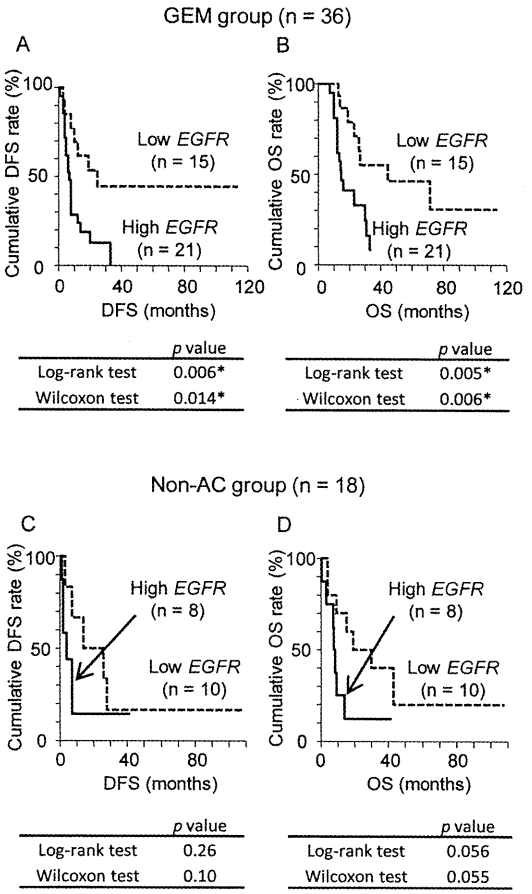

Figure 5. DFS and OS after resection of PDAC with high versus low *EGFR* expression in the GEM (A and B; n=36) and non-AC (C and D; n=18) groups. High *EGFR* mRNA levels were associated with a shorter DFS (A, p=0.068) and a shorter OS (B, p=0.054) in the GEM group. In contrast, there was no significant correlation between *EGFR* expression levels and DFS (C, p=0.30) or OS (D, p=0.07) in the non-AC group. *p<0.05.

did not reach significance in the non-AC group (p=0.07, Fig. 5D). Multivariate analysis of the GEM group (Table IX) showed that OS was significantly dependent on pN status (p=0.024), R factor (p=0.045), and high *EGFR* levels (p=0.023). These data suggest that high *EGFR* expression is a significant predictor for reduced DFS and a significant prognostic indicator for reduced OS, especially in those patients receiving gemcitabine-based AC.

Quantitative analysis of EGFR expression in cells microdissected from cytological specimens. In order to apply this prediction of outcome for PDAC patients receiving gemcitabine-based chemotherapy based on *EGFR* expression levels to a clinical setting, we quantified the *EGFR* mRNA levels in cytological specimens obtained from 20 patients with PDAC who underwent EUS-FNA cytological examination at our institute. Although some samples contained abundant neoplastic cells, most samples contained a large amount of blood and inflammatory cells and scarce clusters of neoplastic cells (Fig. 6A-B). Therefore, we quantified the *EGFR* mRNA levels in the WCP and LCM samples, and then compared the expression levels between the two. We were unable to detect clear differences in *EGFR* mRNA levels in the WCP samples. However, we distinguished higher and lower expression levels of the mRNA in the LCM samples (Fig. 6C). These data suggest that the quantification of *EGFR* expression levels in microdissected neoplastic cells could be a potent tool for

Table V. Multivariate OS analysis (Cox regression model) of conventional prognostic factors and *EGFR* mRNA.

Characteristics	Relative risk	95% Confidence interval	P-value
High *EGFR* levels (>0.058)[a]	1.649	0.958-2.873	0.071
pN category (pN1)	1.671	0.888-3.350	0.114
Residual tumor category (pR1)	3.059	1.762-5.324	<0.0001[b]
Positive vessel invasion	1.784	0.979-3.416	0.059

[a]Cut-off value (0.058) was determined by recursive descent partition analysis of all patients (n=88); [b]p<0.05.

Table VI. Relationship between *EGFR* mRNA expression and various clinicopathological factors in the GEM group (n=36).

Characteristics	*EGFR* mRNA expression[a]		P-value
	High-level group (n=46)	Low-level group (n=42)	
Age			0.176
≥65 years	11 (52.4%)	4 (26.7%)	
<65 years	10 (47.6%)	11 (73.3%)	
Gender			0.736
Male	14 (66.7%)	9 (60.0%)	
Female	7 (33.3%)	6 (40.0%)	
Radiotherapy			0.084
Yes	2 (9.5%)	5 (33.3%)	
No	18 (90.5%)	8 (66.7%)	
pT category			1.000
pT1/pT2	1 (4.8%)	0 (0%)	
pT3/pT4	20 (95.2%)	15 (100%)	
pN category			0.694
pN0	4 (19.0%)	4 (26.7%)	
pN1	17 (81.0%)	11 (73.3%)	
UICC stage			1.000
I	-	-	
II	20 (95.2%)	14 (93.3%)	
III/IV	1 (4.8%)	1 (6.7%)	
Histological grade			0.297
G1	4 (19.0%)	3 (20.0%)	
G2	5 (23.8%)	7 (46.7%)	
G3	12 (57.2%)	5 (33.3%)	
Residual tumor category			0.282
R0	12 (57.2%)	12 (80.0%)	
R1	9 (4.8%)	3 (20.0%)	
Vessel invasion			0.499
Positive	15 (71.4%)	9 (60.0%)	
Negative	6 (28.6%)	6 (40.0%)	
Neural invasion			1.000
Positive	17 (81.0%)	13 (86.7%)	
Negative	4 (19.0%)	2 (13.3%)	

[a]Cut-off value (0.058) was determined by recursive descent partition analysis of all patients (n=88) and the GEM group (n=36).

predicting the outcome of PDAC patients, even when specimens contain abundant contaminated cells.

Discussion

There is increasing evidence showing the usefulness of immunohistochemical analysis of molecular markers, including EGFR, for predicting the clinical outcome of PDAC patients (10,11,13,25,26). Immunohistochemical analysis is a valid method as it shows protein expression. However, the clinical introduction of immunohistochemical assessment for predicting sensitivity to chemotherapeutic agents is still problematic due to difficulties in quantitative measurement (inter-observer variations in interpretation) and the lack of calibrated quantification techniques (27-29). In addition, only 10-20% of patients with PDAC are candidates for curative resection (3). Therefore, the remaining 80–90% of patients with advanced PDAC need cytopathological assessment with EUS-FNA, or pancreatic juice, to predict their sensitivity to chemotherapeutic agents for individualized chemotherapy. The present analysis of *EGFR* mRNA is quantitative (even considering the small amount of specimens available, including cytological specimens). For these reasons, quantitative mRNA analysis of genes associated with tumor sensitivity, or with resistance to anti-tumor agents, could be preferred to immunohistochemical analysis in a clinical setting. Furthermore, we introduced the use of LCM to obtain target cells from EUS-FNA cytological specimens (17). As a result, we found that *EGFR* mRNA levels in microdissected neoplastic cells were easier to distinguish than those in WCP, suggesting that quantification of the expression levels of individual genes in microdissected neoplastic cells could be a potent tool for

Table VII. Univariate survival analysis of conventional prognostic factors and *EGFR* mRNA expression in the GEM group (n=36).

Characteristics	Number of cases	Median DFS (months)	P-value	Median OS (months)	P-value	5-year survival rate
EGFR mRNA expression[a]			0.0068[b]		0.0054[b]	
High	42	7		14.6		8.2%
Low	46	25		45.0		46.0%
Age			0.57		0.92	
≥65 years	17	8		27.0		24.8%
<65 years	23	10		23.0		26.8%
Gender			0.45		0.71	
Male	26	14		27.0		20.9%
Female	14	6		13.7		27.7%
Radiotherapy			0.32		0.24	
Yes	9	12		27.0		34.3%
No	27	8		19.0		12.1%
pT category			0.25		0.09	
pT1/pT2	1	4		10.0		0.0%
pT3/pT4	39	10		26.0		26.1%
pN category			0.0094[b]		0.020[b]	
pN0	9			45.0		46.7%
pN1	31	8		19.0		19.0%
UICC stage			0.62		0.35	
I	0	-		-		-
II	37	8		23.0		27.4%
III/IV	3	2		19.0		0.0%
Histological grade			0.086		0.071	
G1/G2	23	14		31.0		33.3%
G3	17	8		19.0		13.9%
Residual tumor category			0.0004[b]		0.013[b]	
R0	26	19		30.2		39.6%
R1	14	5		13.7		0.0%
Vessel invasion			0.079		0.26	
Positive	26	8		23.0		23.6%
Negative	14	25		31.0		29.2%
Neural invasion			0.56		0.84	
Positive	33	9		26.0		23.5%
Negative	7	8		15.6		50.0%

[a]Cut-off value (0.058) was determined by recursive descent partition analysis of all patients (n=88) and the GEM group (n=36); [b]$p<0.05$.

Table VIII. Multivariate DFS analysis (Cox regression model) of conventional prognostic factors and *EGFR* mRNA expression levels in the GEM group (n=36).

Characteristics	Relative risk	95% Confidence interval	P-value
pN status (pN1)	2.654	0.892-11.41	0.083
Residual tumor category (pR1)	3.197	1.383-7.365	0.0071[b]
High *EGFR* levels (>0.058)[a]	3.016	1.292-7.742	0.010[b]

[a]Cut-off value (0.058) was determined by recursive descent partition analysis of all patients (n=88) and the GEM group (n=36); [b]$p<0.05$.

Table IX. Multivariate OS analysis (Cox regression model) of conventional prognostic factors and *EGFR* mRNA expression levels in the GEM group (n=36).

Characteristics	Relative risk	95% Confidence interval	P-value
pN status (pN1)	3.451	1.157-14.89	0.024[b]
Residual tumor category (pR1)	2.442	1.021-5.858	0.045[b]
High *EGFR* levels (>0.058)[a]	2.882	1.154-8.194	0.023[b]

[a]Cut-off value (0.058) was determined by recursive descent partition analysis of all patients (n=88) and the GEM group (n=36); [b]p<0.05.

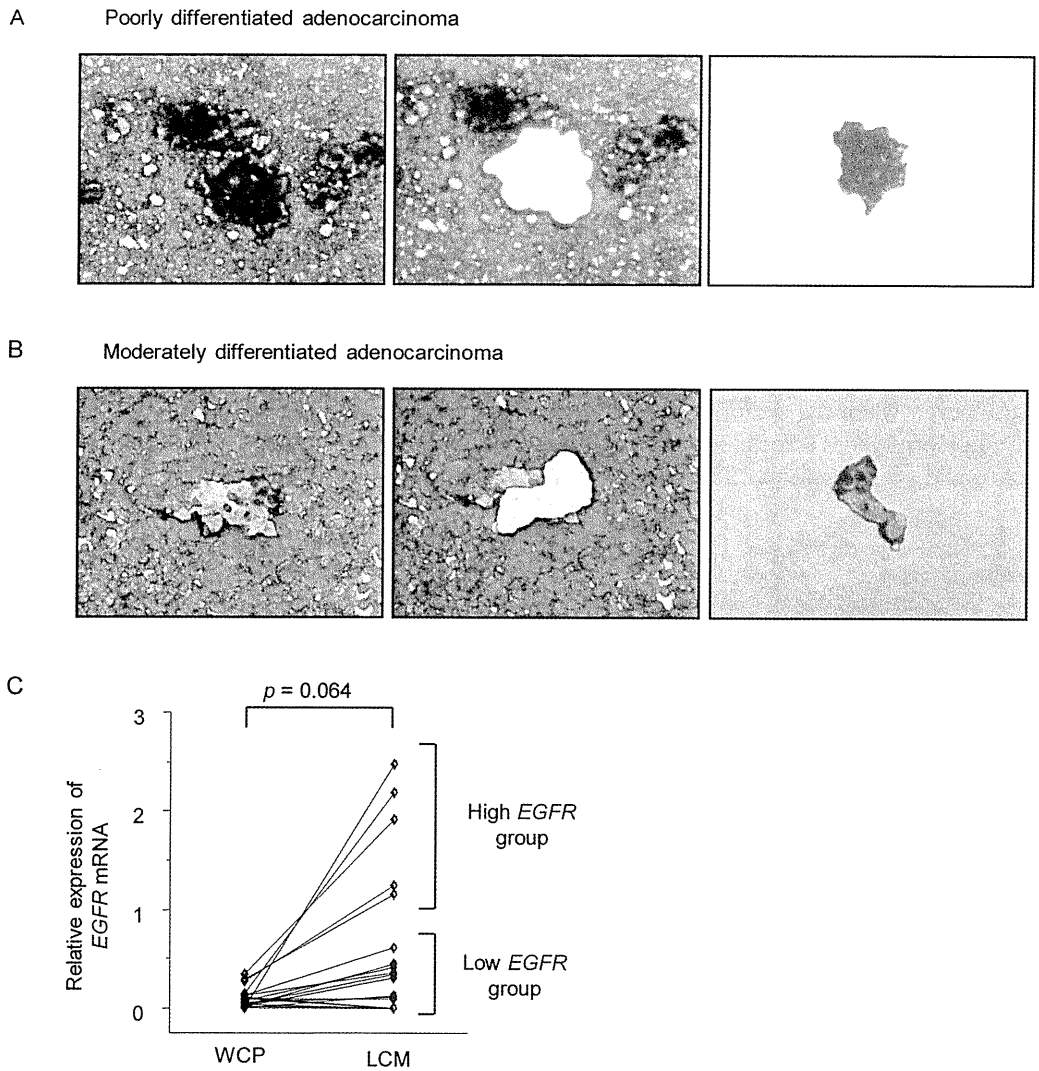

Figure 6. Quantitative analyses of *EGFR* mRNA in EUS-FNA cytological specimens. Representative micrographs of cytological specimens obtained from patients with PDAC who underwent EUS-FNA cytological examination (A and B). Most samples contained a large amount of blood and inflammatory cells with scarce clusters of neoplastic cells. (C) Quantitative analysis of *EGFR* in EUS-FNA cytological specimens (n=20). Although we did not detect clear changes in expression levels in the WCP samples, we distinguished samples having higher and lower *EGFR* expression levels in the microdissected neoplastic cells (C).

predicting sensitivity to anti-tumor agents, even when specimens contain contaminated cells. However, further investigations, including prospective studies, are required before this approach can be introduced into the clinical setting.

As EGFR plays a crucial role in controlling the activity of the Ras/MAPK signaling pathway (8,9), great efforts have been made to develop strategies targeting EGFR (30). In xenograft models of pancreatic cancer, the combination of gemcitabine and EGFR-targeted therapy significantly inhibited lymph node and liver metastases and improved OS (16). A randomized, placebo-controlled phase III trial comparing erlotinib, an EGFR tyrosine kinase inhibitor (TKI), plus gemcitabine to gemcitabine alone in patients with locally advanced or metastatic pancreatic cancer, demonstrated that